

Quantum kinetics of an open system in the presence of periodic refocusing fields

Leonid P. Pryadko and Pinaki Sengupta*

Department of Physics, University of California, Riverside, California 92521, USA

(Received 30 September 2005; revised manuscript received 20 December 2005; published 24 February 2006)

We consider quantum kinetics of an open quantum system in the presence of periodic fields designed to suppress the internal evolution and shield the system from a generic low-frequency environment (refocusing or dynamical decoupling in an application to multiqubit systems). Assuming that the refocusing has order K , that is, for a frozen environment the cumulant expansion of the evolution operator over the period τ begins with the term $\sim \tau^{K+1}$, we trace the associated cancellations in the kernel of the quantum kinetic equation in the Floquet formalism and characterize the remaining decoherence processes.

DOI: [10.1103/PhysRevB.73.085321](https://doi.org/10.1103/PhysRevB.73.085321)

PACS number(s): 03.67.Pp, 03.67.Lx, 82.56.Jn, 75.10.Pq

I. INTRODUCTION

The evolution of a quantum system subject to external time-dependent fields is a well-studied problem that goes all the way to the origins of quantum mechanics. However, driven dynamics in conventional atomic physics rarely involves dynamical interference patterns as intricate as those that occur, e.g., in multidimensional nuclear magnetic resonance (NMR) experiments and other applications of coherent control, where precisely shaped and timed signals are used to steer the quantum evolution of the system. One such control method¹⁻³ originally developed in NMR is a pulse-based technique known as dynamical recoupling (also, “bang-bang,” in the case of hard, δ -function-like pulses). In the simplest setup, the system is a collection of individually controlled weakly coupled parts (e.g., qubits). Individual qubits undergo a rapid forced precession, while the overall long-time evolution of the system is governed by the effective Hamiltonian averaged over their precession. For example, the interaction $J\sigma_1^x\sigma_2^z$ between the two qubits is canceled on average if one of them is rapidly precessing around the x axis. Such a cancellation of the quantum evolution is called “dynamical decoupling” or “refocusing;” it is obviously related to the spin-echo experiment.⁴

An exciting thing about dynamical decoupling is its universality: one does not need to know the magnitude of the interaction precisely to cancel it. Moreover, with sufficiently fast pulse rate one can also cancel the evolution due to slowly varying external perturbations, in effect suppressing the decoherence caused by the environment.⁵⁻¹⁹ A general analysis of such methods was limited to numerics and/or the idealized δ -function-like “hard” pulses whose duration was either ignored or assumed small. In real experiments (especially in solid-state systems), very short pulses are impractical because they tend to couple to degrees of freedom in wide spectral ranges which leads to signal distortions and heating.²⁰ Besides, from the previous studies it is hard to judge whether high-order refocusing sequences involving more intricate cancellation (dynamical destructive interference) of the quantum dynamics have a real advantage in suppressing the decoherence.

The goal of this work is to construct a general theory of quantum kinetics of open systems in the presence of periodic

refocusing fields designed to suppress the internal evolution and decouple the system from outside degrees of freedom. We describe the evolution of the density matrix of such systems, with weak internal and thermal bath couplings, in the approximation of master (quantum kinetic) equation in the Floquet formalism. The kinetics of the system is treated in a non-Markovian approximation,²¹⁻²⁴ which is essential to trace the decoherence suppression with the bath “slow” on the scale of the driven dynamics.

Our analysis begins with the assumption that the period- τ control fields provide order- K refocusing for the system with the bath frozen. That is, if we replace the operators for the external degrees of freedom by c numbers, the cumulant expansion of the evolution operator in powers of thus modified internal Hamiltonian begins with the terms of order $\sim \tau^{K+1}$. The control fields are assumed to be strong and we treat them exactly. We trace the cancellations associated with refocusing in the kernel of the quantum kinetic equation (QKE), which describes the dissipative dynamics of the density matrix of the system with the bath present, and characterize the remaining decoherence processes. We illustrate the general analytic results derived for orders $K \leq 2$, which is the accuracy of the employed QKE, with the numerical simulations of dynamics of a single spin in the presence of a classical fluctuating magnetic field.

Our results can be summarized as follows. Generally, for a weakly coupled system weakly interacting with slow degrees of freedom (thermal bath) with the correlation time τ_0 , the decoherence is due to dissipative processes (resonant decay) which create excitation(s) in the environment, as well as reactive processes which result in dephasing, or scrambling of the phase of the system. The associated decoherence rate is proportional to the square of the coupling matrix element and the correlation time τ_0 , see Eq. (30). As a result of forced precession of the system caused by the control fields, the effective environment seen by the system is modulated out of resonance, which may entirely suppress the state decay.^{25,26} Only first-order ($K=1$) refocusing is necessary to achieve such an effect. We show that, in addition, the rate of reactive processes is reduced by a factor of τ/τ_0 [Eq. (41)], where the period of the refocusing sequence, τ , is assumed to be smaller than τ_0 . With second-order refocusing, $K=2$, the decoherence rate is additionally suppressed [Eq. (44)], and with

time-reversal invariant bath couplings it may even become exponentially small in this parameter (in which case it will be determined by terms of higher order in bath coupling, beyond the accuracy of our QKE).

In addition to the decoherence rates which characterize the exponential decay of quantum correlations with time, we also analyze the corresponding prefactor, which determines the initial decoherence.²⁷ While for generic refocusing sequences with $K \geq 1$ the initial decoherence is quadratic in τ and does not scale with the thermal bath correlation time τ_0 ; we show that for symmetric pulse sequences it is reduced by an additional power of (τ/τ_0) .

Our results extend the well-established theory²⁸ of the kinetics of few-level systems in the rf field to cases involving a more intricate cancellation (dynamical destructive interference) of the quantum dynamics characteristic of higher-order refocusing sequences. They put in perspective the previous analyses of decoherence in the presence of hard-pulse sequences,⁵⁻¹⁹ establish a firm basis for future studies of decoherence scaling in large driven qubit systems (with and without long-range coupling due to long-wavelength phonons which may be correlated²⁹ between distant qubits, contrary to a common assumption in the quantum error-correction theory³⁰), and present an efficient alternative to optimum control techniques based directly on the master equation.³¹⁻³³

Some of the results regarding decoherence suppression in the presence of higher-order refocusing sequences were announced previously,²⁰ as a justification for developing a technique for designing higher-order pulses and pulse sequences.

II. PROBLEM SETUP

A. Hamiltonian of the system

We consider an N -level open system with the Hamiltonian

$$H = H_C(t) + H_S + H_{Sb} + H_b, \quad (1)$$

where the oscillator bath Hamiltonian $H_b = \sum_{\mu} \omega_{\mu} a_{\mu}^{\dagger} a_{\mu}$ has the usual form, while the control Hamiltonian

$$H_C \equiv \frac{1}{2} \sum_{\alpha} V_{\alpha}(t) \Sigma_{\alpha}, \quad (2)$$

the system Hamiltonian

$$H_S \equiv \frac{1}{2} \sum_{\alpha} J_{\alpha} \Sigma_{\alpha}, \quad (3)$$

and the system-bath coupling Hamiltonian

$$H_{Sb} \equiv \frac{1}{2} \sum_{\alpha} b_{\alpha} \Sigma_{\alpha}, \quad b_{\alpha} = \sum_{\mu} \frac{f_{\alpha\mu} a_{\mu} + f_{\alpha\mu}^{*} a_{\mu}^{\dagger}}{(2m_{\mu} \omega_{\mu})^{1/2}}, \quad (4)$$

are expressed in terms of $N \times N$ Hermitian matrices Σ_{α} , $\alpha = 0, \dots, N^2 - 1$, normalized so that $\text{Tr}(\Sigma_{\alpha} \Sigma_{\beta}) = N \delta_{\alpha\beta}$. It is convenient to specify explicitly $\Sigma_0 = 1$, choose the remaining matrices traceless, and define the algebra via the commutators and the anticommutators,

$$[\Sigma_{\alpha}, \Sigma_{\beta}] = 2i C_{\alpha\beta}^{\gamma} \Sigma_{\gamma}, \quad \{\Sigma_{\alpha}, \Sigma_{\beta}\} = 2B_{\alpha\beta}^{\gamma} \Sigma_{\gamma}. \quad (5)$$

For example, for a single qubit (spin) $N=2$, we can choose $\Sigma_{\alpha} \equiv \sigma_{\alpha}$, $\alpha=0, \dots, 3$, in terms of the unit matrix $\sigma_0 \equiv 1$ and the three Pauli matrices, in which case the net coefficients $B_{\nu}(t) = V_{\nu}(t) + J_{\nu} + b_{\nu}$, $\nu=1, 2, 3$, can be interpreted as the components of the time-dependent magnetic field acting on the spin.

Similarly, for two-qubit systems the full set can be chosen in terms of the direct products $\sigma_i \otimes \sigma_j$, $i, j=0, 1, 2, 3$. In this case, the coefficients in front of the single-spin operators $\sigma_{1\nu} \equiv \sigma_{\nu} \otimes \sigma_0$ and $\sigma_{2\nu} \equiv \sigma_0 \otimes \sigma_{\nu}$ can be interpreted as the components of the magnetic fields acting on the corresponding spin, while the two-spin operators $\sigma_{\nu} \otimes \sigma_{\rho}$ describe spin couplings.

The same matrices will be used to parametrize the density matrix of the system,

$$\rho = \frac{1}{N} \left(\Sigma_0 + \sum_{\alpha \geq 1} R_{\alpha} \Sigma_{\alpha} \right). \quad (6)$$

The normalization is chosen so that $\text{Tr} \rho = 1$. Also, for a pure state, $\rho^2 = \rho$, we have $R^2 \equiv (R_{\alpha})^2 = N - 1$ (summation implicit), while for the fully mixed state $R^2 = 0$.

Generally, only a few of all N^2 allowed terms are expected to be present in the Hamiltonian. Particularly, for n -qubit systems with $N=2^n$, it is common to have single-qubit controlling fields $V_{l\nu}$, $l=1, \dots, n$, while the couplings (both intrinsic ones, J_{α} , and bath, b_{α}) can be one-, two-, or multiparticle as physically appropriate.

B. Dynamical decoupling in a closed system

Here we consider an auxiliary control problem for the system (1) with the thermal bath operators b_{α} in Eq. (4) replaced by constant numbers, which in effect modifies the coefficients in the system Hamiltonian (3). The control goal is to suppress the unitary evolution with thus modified Hamiltonian H_S as fully as possible. Unless the fields $V_{\alpha}(t)$ are specified to exactly compensate the Hamiltonian H_S (which is never practical), the refocusing can only be achieved at some discrete set of time moments $t_0=0$, $t_1 = \tau, \dots$. The unitary evolution over the refocusing interval τ is commonly analyzed in terms of the effective Hamiltonian theory, a perturbative scheme based on the cumulant (Magnus) expansion for the evolution operator.^{34,35} The expansion is done around the evolution in the applied controlling fields [Hamiltonian $H_C(t)$], while the system Hamiltonian H_S is treated perturbatively. Obviously, this implies that the controlling Hamiltonian dominates the evolution.

Explicitly, consider the evolution operator $U(t)$,

$$\dot{U}(t) = -i[H_C(t) + H_S]U(t), \quad U(0) = 1. \quad (7)$$

As usual, the time-dependent perturbation theory is introduced by separating out the bare evolution operator,

$$U(t) = U_0(t) \mathcal{R}(t), \quad \dot{U}_0(t) = -iH_C(t)U_0(t). \quad (8)$$

Then, the operator $\mathcal{R}(t)$ obeys the equation

$$\dot{\mathcal{R}}(t) = -iH_S(t)\mathcal{R}(t), \quad H_S(t) \equiv U_0^\dagger(t)H_S U_0(t), \quad (9)$$

which can be iterated to construct the standard expansion $\mathcal{R}(t) = 1 + \mathcal{R}_1(t) + \mathcal{R}_2(t) + \dots$ in powers of (tH_S) ,

$$\dot{\mathcal{R}}_{n+1}(t) = -iH_S(t)\mathcal{R}_n(t), \quad \mathcal{R}_0(t) = 1. \quad (10)$$

The standard Magnus expansion is readily obtained by integrating Eqs. (10) formally and rewriting the result in terms of cumulants,

$$\mathcal{R}(t) = \exp(C_1(t) + C_2(t) + \dots), \quad (11)$$

$$C_1(t) = -i \int_0^t dt_1 H_S(t_1), \quad (12)$$

$$C_2(t) = -\frac{1}{2} \int_0^t dt_2 \int_0^{t_2} dt_1 [H_S(t_1), H_S(t_2)], \dots \quad (13)$$

Generally, the term C_k contains a k -fold integration of the commutators of the rotating-frame Hamiltonian $H_S(t_i)$ at different time moments t_i and has an order $(tH_S)^k$. For a given Hamiltonian H_S , order- K refocusing is characterized by a vanishing of the terms C_k of order $k \leq K$ at the given time moment $t = \tau$. This is equivalent to the condition $\mathcal{R}_k(\tau) = 0$ for $k = 1, \dots, K$. The latter matrices can be efficiently evaluated numerically, which gives a systematic method for an analysis and optimization of the controlled dynamics in high orders of the cumulant expansion.²⁰

In terms of the matrices Σ_α , the unitary transformation generated by the control fields amounts to a rotation,

$$U_0(t)\Sigma_\alpha U_0^\dagger(t) \equiv Q_{\alpha\beta}(t)\Sigma_\beta, \quad (14)$$

where the matrix $\hat{Q}(t)$ is orthogonal, $\hat{Q}^{\text{tr}} = \hat{Q}^{-1}$. We assume the matrix to be periodic with the refocusing period τ , $\hat{Q}(t) = \hat{Q}(t + \tau)$, which will be referred to as the ‘‘zeroth order’’ refocusing condition. This condition is nontrivial; it does not reduce to the periodicity of the control fields $V_\alpha(t)$.

The periodicity of the real-valued matrix $\hat{Q}(t)$ implies the Fourier expansion with the frequencies $\Omega_m \equiv 2\pi m / \tau$,

$$\hat{Q}(t) = \sum_m \hat{A}_m e^{i\Omega_m t}, \quad \hat{A}_{-m} = \hat{A}_m^*. \quad (15)$$

From orthogonality $\hat{Q}(t)\hat{Q}^{\text{tr}}(t) = \hat{1}$ we have

$$\sum_k \hat{A}_k \hat{A}_{m-k}^{\text{tr}} = \delta_{m,0} \hat{1}. \quad (16)$$

With these definitions, it is easy to rewrite the first two refocusing conditions in algebraic form. Specifically,

$$iC_1(\tau) = \frac{1}{2} J_\alpha \Sigma_\beta \int_0^\tau dt Q_{\alpha\beta}(t),$$

and the first-order refocusing condition $C_1(\tau) = 0$ is

$$[\hat{A}_0^{\text{tr}}]_{\beta\alpha} J_\alpha = 0, \quad \text{or just } \hat{A}_0^{\text{tr}} J = 0, \quad (17)$$

where in the second form of the expression we treated the coefficients J_α as a column vector.

Performing the double integration in Eq. (13) in the assumption that the first-order refocusing condition is satisfied, we have for the second-order refocusing, $C_2(\tau) = 0$,

$$C_{\alpha\beta}^\gamma \sum_{m \neq 0} \frac{[\hat{A}_{-m}^{\text{tr}} J J^{\text{tr}} \hat{A}_m]_{\alpha\beta}}{i\Omega_m} = 0, \quad (18)$$

where the coefficients $C_{\alpha\beta}^\gamma$ define the commutators, see Eq. (5). We note that the sum in Eq. (18) is antisymmetric with respect to indices α, β , and an analogous condition with the symmetric coefficients $B_{\alpha\beta}^\gamma$ [which define anticommutators in Eq. (5)] is trivially satisfied.

III. QUANTUM KINETICS

A. Quantum kinetic equation in rotating frame

In this work we consider slow (on the scale of the refocusing period τ) environment, which makes it necessary to consider quantum dynamics of the system outside the commonly used Markovian approximation. We write the master equation as^{21–24}

$$\dot{\rho}(t) = -i[\langle H_1(t) \rangle, \rho(t)] - \int_0^t dt' \text{Tr}_b[\delta H_1(t), [\delta H_1(t'), \rho(t') \rho_b]], \quad (19)$$

where $\langle H_1(t) \rangle \equiv \text{Tr}_b(H_1(t) \rho_b)$ and $\delta H_1(t) \equiv H_1(t) - \langle H_1(t) \rangle$. Here $H_1(t)$ is the interaction representation of the perturbation Hamiltonian $H_1 \equiv H_S + H_{Sb}$ [see Eq. (1)] in the rotating frame generated by the control and the thermal bath parts of the Hamiltonian, $H_0 \equiv H_C + H_b$, and the bath is assumed to be in thermal equilibrium, $\rho_b \equiv \exp(-\beta H_b) / Z$, $Z \equiv \text{Tr}_b \exp(-\beta H_b)$.

With the definitions (3) and (4) the average perturbation Hamiltonian in the first term of the QKE (19) is given just by Eq. (9),

$$\langle H_1(t) \rangle = H_S(t) = \frac{1}{2} [\hat{Q}^{\text{tr}}(t) J]_\alpha \Sigma_\alpha, \quad (20)$$

while the corresponding fluctuating part is

$$\delta H_1(t) = H_{Sb}(t) = \frac{1}{2} Q_{\beta\alpha}^{\text{tr}}(t) b_\alpha(t) \Sigma_\beta, \quad (21)$$

where the oscillator fields in the interaction representation $b_\alpha(t)$ are given by Eq. (4) with the replacement $a_\mu \rightarrow a_\mu e^{i\omega_\mu t}$.

The second term in the right-hand side of the QKE (19) is evaluated in terms of two correlators,

$$\mathcal{F}_{\alpha\beta}(t - t') = \text{Tr}_b\{b_\alpha(t) b_\beta(t') \rho_b\}, \quad (22)$$

$$\bar{\mathcal{F}}_{\alpha\beta}(t - t') = \text{Tr}_b\{b_\alpha(t) \rho_b b_\beta(t')\}, \quad (23)$$

which in turn can be conveniently expressed in terms of the spectral coupling matrix (function)

$$F_{\alpha\beta}(\omega) \equiv \frac{\pi}{2} \sum_{\mu} \frac{f_{\alpha\mu} f_{\beta\mu}^*}{m\omega_{\mu}} \delta(\omega - \omega_{\mu}). \quad (24)$$

The fastest response time of the environment is characterized by the largest frequency of an oscillator present in the system. We will introduce the cutoff frequency ω_c , such that $F_{\alpha\beta}(\omega)$ is only nonzero for $\omega < \omega_c$. In addition, we will characterize the bath with a possibly slower ‘‘correlation time’’ τ_0 , which describes the width of typical features of the spectral coupling function $F_{\alpha\beta}(\omega)$.

Operators $b_{\alpha}(t)$ are Hermitian, thus $\hat{\mathcal{F}}^{\dagger}(t) = \hat{\mathcal{F}}(-t)$. An explicit calculation gives $\bar{\mathcal{F}}_{\alpha\beta}(t) = \mathcal{F}_{\alpha\beta}^*(t)$, and

$$\hat{\mathcal{F}}(t) = \int_0^{\infty} \frac{d\omega}{\pi} [\hat{F}(\omega)(n_{\omega} + 1)e^{i\omega t} + \hat{F}^*(\omega)n_{\omega}e^{-i\omega t}]. \quad (25)$$

It is convenient to split this correlator into real and imaginary parts, $\hat{\mathcal{F}}(t) = \hat{\mathcal{F}}_1(t) + i\hat{\mathcal{F}}_2(t)$, where the real-valued matrices $\hat{\mathcal{F}}_1(t)$ and $\hat{\mathcal{F}}_2(t)$ are, respectively, symmetric and antisymmetric. The QKE (19) becomes

$$\begin{aligned} \dot{\rho}(t) = & -\frac{i}{2} Q_{\alpha\beta}^{\text{tr}}(t) J_{\beta} [\Sigma_{\alpha}, \rho(t)] \\ & - \frac{1}{4} \int_0^t dt' [\hat{Q}^{\text{tr}}(t) \hat{\mathcal{F}}_1(t-t') \hat{Q}(t')]_{\alpha\beta} [\Sigma_{\alpha}, [\Sigma_{\beta}, \rho(t')]] \\ & - \frac{i}{4} \int_0^t dt' [\hat{Q}^{\text{tr}}(t) \hat{\mathcal{F}}_2(t-t') \hat{Q}(t')]_{\alpha\beta} [\Sigma_{\alpha}, \{\Sigma_{\beta}, \rho(t')\}]. \end{aligned} \quad (26)$$

This can be further simplified with the help of the definitions (5) and (6):

$$\begin{aligned} \dot{R}_{\gamma}(t) = & Q_{\alpha\beta}^{\text{tr}}(t) J_{\beta} C_{\alpha\delta}^{\gamma} R_{\delta}(t) + \int_0^t dt' [\hat{Q}^{\text{tr}}(t) \hat{\mathcal{F}}_1(t-t') \hat{Q}(t')]_{\alpha\beta} \\ & \times C_{\alpha\alpha'}^{\gamma} C_{\beta\delta}^{\alpha'} R_{\delta}(t') + \int_0^t dt' [\hat{Q}^{\text{tr}}(t) \hat{\mathcal{F}}_2(t-t') \hat{Q}(t')]_{\alpha\beta} \\ & \times C_{\alpha\alpha'}^{\gamma} B_{\beta\delta}^{\alpha'} R_{\delta}(t') + \int_0^t dt' [\hat{Q}^{\text{tr}}(t) \hat{\mathcal{F}}_2(t-t') \hat{Q}(t')]_{\alpha\beta} C_{\alpha\beta}^{\gamma}, \end{aligned} \quad (27)$$

where the last term comes from the (time-independent) part of the density matrix (6) proportional to $\Sigma_0 \equiv \mathbb{1}$. This term is responsible for establishing the equilibrium at large t (dynamical equilibrium with refocusing).

We note that the structure of the QKE [in particular, Eqs. (25) and (27)] remains the same even if the nature of the thermal bath coupling is changed (e.g., by adding nonlinear oscillator couplings) as long as the bath remains in thermal equilibrium. In such cases, the only change would be a renormalization of the average Hamiltonian (20) and of the coupling matrix (24).

B. Kinetics in the absence of control

In the absence of refocusing, $\hat{Q}(t) = \hat{1}$, the QKE (27) does not depend on time explicitly, and it can be solved with the help of the Laplace transform [denoted with tilde, $f(t) \rightarrow \tilde{f}(p)$],

$$p\tilde{R}_{\gamma}(p) - R_{\gamma}(0) = \Pi_{\gamma\delta}(p)\tilde{R}_{\delta}(p) + \tilde{\mathcal{F}}_{2,\alpha\beta}(p)C_{\alpha\beta}^{\gamma}, \quad (28)$$

where the kernel

$$\Pi_{\gamma\delta} = J_{\alpha} C_{\alpha\delta}^{\gamma} + C_{\alpha\alpha'}^{\gamma} (\tilde{\mathcal{F}}_{1,\alpha\beta}(p) C_{\beta\delta}^{\alpha'} + \tilde{\mathcal{F}}_{2,\alpha\beta}(p) B_{\beta\delta}^{\alpha'}) \quad (29)$$

incorporates the first three terms on the right-hand side of Eq. (27).

The dissipative dynamics of the system is defined by the singularities of the matrix $[\hat{1}p - \hat{\Pi}(p)]^{-1}$, whose location on the complex plane p determine the spectrum of the decoherence rates. For long-time dynamics, only the singularities close to the imaginary axis are relevant. With both the intrinsic interactions J and bath couplings \mathcal{F} weak on the scale of the bath correlation time τ_0 , a good accuracy can be obtained by setting $p \rightarrow 0$ in the QKE kernel $\hat{\Pi}(p)$ [Eq. (29)], which is equivalent to the Markovian bath approximation. Then, the real parts of the eigenvalues of the matrix $\hat{\Pi}(0)$ will determine the spectrum of the decoherence rates. If we bunch together all processes causing the evolution of the density matrix, the maximum decoherence rate can be estimated as

$$\Gamma_0 \sim \max[J, \Delta(0)\tau_0], \quad (30)$$

where $\Delta(t) \equiv \|\hat{\mathcal{F}}(t)\|$ is a norm of the correlator matrix (25), and τ_0 is the bath correlation time introduced below Eq. (24).

C. Quantum kinetics in Floquet formalism

The full kinetic equation (27) in the presence of refocusing can also be analyzed with the help of the Laplace transformation, but in this case the structure of the solution is complicated by the presence of the time-dependent rotation matrices $\hat{Q}^{\text{tr}}(t)$, $\hat{Q}(t')$. Assuming these are periodic (‘‘zeroth-order’’ refocusing condition), we use the expansion (15) to obtain [cf. Eq. (28)]

$$p\tilde{R}_{\gamma}(p) = \sum_m \Pi_{m,\gamma\delta}(p)\tilde{R}_{\delta}(p - i\Omega_m) + r_{\gamma}(p), \quad (31)$$

where the kernel with the frequency transfer Ω_m is

$$\begin{aligned} \Pi_{m,\gamma\delta}(p) = & (A_m^{\text{tr}})_{\alpha\beta} J_{\beta} C_{\alpha\delta}^{\gamma} \\ & + C_{\alpha\alpha'}^{\gamma} \sum_{m'} \int \frac{d\omega}{2\pi} \left\{ \frac{[\hat{A}_{m-m'}^{\text{tr}} \tilde{\mathcal{F}}_1(\omega) \hat{A}_{m'}]_{\alpha\beta}}{p - i\omega - i\Omega_{m-m'}} C_{\beta\delta}^{\alpha'} \right. \\ & \left. + \frac{[\hat{A}_{m-m'}^{\text{tr}} \tilde{\mathcal{F}}_2(\omega) \hat{A}_{m'}]_{\alpha\beta}}{p - i\omega - i\Omega_{m-m'}} B_{\beta\delta}^{\alpha'} \right\}, \end{aligned} \quad (32)$$

and the second term on the right-hand side of Eq. (31) is

$$r_{\gamma}(p) = R_{\gamma}(0) + \sum_m \frac{s_{m,\gamma}(p)}{p - i\Omega_m}, \quad (33)$$

$$s_{m,\gamma}(p) \equiv \sum_{m'} \int \frac{d\omega}{2\pi} \frac{[\hat{A}_{m-m'}^{\text{tr}} \tilde{\mathcal{F}}_2(\omega) \hat{A}_{m'}]_{\alpha\beta} C_{\alpha\beta}^{\gamma}}{p - i\omega - i\Omega_{m-m'}}. \quad (34)$$

The obtained expression (31) is a set of functional equations for the Laplace-transformed matrix elements $\tilde{R}_\gamma(p)$ of the density matrix (6). We iterate these equations to obtain a formal series in powers of $\hat{\Pi}_m$,

$$\begin{aligned} \tilde{R}(p) &= \frac{r(p)}{p} + \sum_{m_1} \frac{\hat{\Pi}_{m_1}(p)}{p} \frac{r(p_1)}{p_1} \\ &+ \sum_{m_1, m_2} \frac{\hat{\Pi}_{m_1}(p)}{p} \frac{\hat{\Pi}_{m_2-m_1}(p_1)}{p_1} \frac{r(p_2)}{p_2} \\ &+ \sum_{\{m\}} \frac{\hat{\Pi}_{m_1}(p)}{p} \frac{\hat{\Pi}_{m_2-m_1}(p_1)}{p_1} \frac{\hat{\Pi}_{m_3-m_2}(p_2)}{p_2} \frac{r(p_3)}{p_3} + \dots, \end{aligned} \quad (35)$$

where $p_n \equiv p - i\Omega_{m_n}$. Generally, long-time behavior corresponds to small values of p , while that near the ends of the refocusing interval is governed by values of p close to any $i\Omega_l$, resulting in an asymptotic decomposition, $R_\alpha(t) = \sum_l R_\alpha^{[l]} e^{i\Omega_l t - \gamma t}$. We will analyze the terms with different l separately, beginning with $l \neq 0$.

To evaluate the dynamics around a given frequency Ω_l , we need to carefully account for the terms singular near $p = i\Omega_l$. To this end, denote the sum of all nonsingular (for small $p - i\Omega_l$ with given l) terms connecting the terms with the denominators $p' \equiv p - i\Omega_{l'}$ and $p'' \equiv p - i\Omega_{l''}$,

$$\begin{aligned} \hat{\Pi}_{l', l''}^{[l]}(p) &\equiv \hat{\Pi}_{l''-l'}(p') + \sum_{m_1 \neq l} \hat{\Pi}_{m_1-l'}(p') \frac{\hat{\Pi}_{l''-m_1}(p_1)}{p_1} \\ &+ \sum_{m_1, m_2 \neq l} \hat{\Pi}_{m_1-l'}(p') \frac{\hat{\Pi}_{m_2-m_1}(p_1)}{p_1} \frac{\hat{\Pi}_{l''-m_2}(p_2)}{p_2} + \dots. \end{aligned} \quad (36)$$

Note that this definition implies

$$\hat{\Pi}_{l', l''}^{[l]}(p) = \hat{\Pi}_{l'-l, l''-l}^{[0]}(p - i\Omega_l). \quad (37)$$

The entire series near $p = i\Omega_l$, $l \neq 0$, can now be written as

$$\begin{aligned} \tilde{R}^{[l]}(p) &= \frac{r(p)}{p} + \frac{\hat{\Pi}_{0,l}^{[l]}(p)}{p} [p - i\Omega_l - \hat{\Pi}_{l,l}^{[l]}(p)]^{-1} \\ &\times \left[r(p - i\Omega_l) + \sum_{m \neq l} \hat{\Pi}_{l,m}^{[l]}(p) \frac{r(p - i\Omega_m)}{p - i\Omega_m} \right], \end{aligned} \quad (38)$$

while near $p=0$ it is

$$\begin{aligned} \tilde{R}^{[0]}(p) &= (p - \hat{\Pi}_{0,0}^{[0]}(p))^{-1} \left[R(0) + \sum_m \frac{s_m(p)}{p - i\Omega_m} \right. \\ &+ \sum_{m \neq 0} \frac{\hat{\Pi}_{0,m}^{[0]}(p)}{p - i\Omega_m} R(0) \\ &\left. + \sum_{m \neq 0} \frac{\hat{\Pi}_{0,m}^{[0]}(p)}{p - i\Omega_m} \sum_{m'} \frac{s_{m'}(p - i\Omega_m)}{p - i\Omega_m - i\Omega_{m'}} \right], \end{aligned} \quad (39)$$

where Eq. (33) for $r(p)$ was substituted for completeness.

The analysis of the obtained expressions is dramatically simplified with at least order-one refocusing, as long as the couplings J_α and the bath couplings $\hat{\mathcal{F}}(t)$ are weak on the refocusing time scale τ , which is assumed to be short on the scale of the bath correlation time τ_0 , $\tau \ll \tau_0$.

Indeed, the universal *order-one refocusing* condition Eq. (17) implies the disappearance of the average Hamiltonian regardless of the specific values of the couplings J_α . Thus, in the kernel $\hat{\Pi}_m(p)$ [Eq. (32)] with $m=0$, the first term disappears completely. Furthermore, if we assume that the set of the fluctuating fields b_α in the bath coupling Hamiltonian (4) is the same as that of the constant parameters J_α in the system Hamiltonian (3), the terms with resonant denominators ($m-m'=0$) inside the ω integrals in Eqs. (32) and (34) will also be suppressed. Then, for small $|p|$, the resonant contribution to these expressions will be limited by $|\omega| \geq \Omega$, which by assumption is far out in the tail region of the spectral coupling function (24). The remaining nonresonant contributions can be calculated by expanding in powers of ω under the integrals.

In particular, the spectrum of the dissipation rates is determined by the positions of the singularities of the QKE resolvent, $(p - \hat{\Pi}_{0,0}^{[0]}(p))^{-1}$ [see Eq. (39)]. At small coupling these are determined by the eigenvalues of the matrix $\hat{\Pi}_{0,0}^{[0]}(p=0)$ [Eq. (36)]. To the quadratic order in powers of the perturbing Hamiltonian, with the help of Eq. (32), we have

$$\begin{aligned} [\hat{\Pi}_{0,0}^{[0]}(p)]_{\gamma\delta} &= \sum_{m \neq 0} \frac{[\hat{A}_{-m}^{\text{tr}} J J^{\text{tr}} \hat{A}_m]_{\alpha\beta} C_{\alpha\alpha'}^{\gamma} C_{\beta\delta}^{\alpha'}}{p - i\Omega_{-m}} \\ &+ \sum_{m \neq 0} \sum_{k \geq 0} C_{\alpha\alpha'}^{\gamma} \left\{ \frac{[\hat{A}_{-m}^{\text{tr}} \hat{\mathcal{F}}_1^{(k)}(0) \hat{A}_m]_{\alpha\beta} C_{\beta\delta}^{\alpha'}}{(p - i\Omega_{-m})^{k+1}} C_{\beta\delta}^{\alpha'} \right. \\ &\left. + \frac{[\hat{A}_{-m}^{\text{tr}} \hat{\mathcal{F}}_2^{(k)}(0) \hat{A}_m]_{\alpha\beta} B_{\beta\delta}^{\alpha'}}{(p - i\Omega_{-m})^{k+1}} \right\}, \end{aligned} \quad (40)$$

where $\hat{\mathcal{F}}^{(k)}(0)$ is the k th derivative of the correlator $\hat{\mathcal{F}}(t)$ [Eq. (25)] evaluated at $t=0$. The corresponding maximum decoherence rate with order-one refocusing (which is determined by *reactive* nonresonant processes) can be estimated as

$$\Gamma_1 \sim \max[J^2 \tau, \Delta(0) \tau], \quad (41)$$

where $\Delta(t) \equiv \|\hat{\mathcal{F}}(t)\|$ was defined below Eq. (30). Here the first expression comes from the first term in Eq. (40) and originates from the noncompensated evolution due to the system Hamiltonian (3), while the second term is an estimate

of the leading order of the derivative expansion in Eq. (40). The presence of the instantaneous correlator can be interpreted as an effect of nearly static fluctuations of the coefficients J_α due to the presence of the bath. Comparing with the corresponding expression in the absence of refocusing, we note that already with the first-order refocusing the decoherence rate is reduced as long as the refocusing is fast enough, $\tau/\tau_0 \ll 1$, $J\tau \ll 1$.

With the *second-order refocusing*, Eq. (18), all the evolution to quadratic order in J should be compensated. To demonstrate this cancellation explicitly for the first term of Eq. (40) with $p=0$, we denote

$$\mathcal{M}_{\alpha\beta} \equiv \sum_{m \neq 0} \frac{[\hat{A}_{-m}^{\text{tr}} J J^{\text{tr}} \hat{A}_m]_{\alpha\beta}}{-i\Omega_{-m}}, \quad \hat{\mathcal{M}}^{\text{tr}} = -\hat{\mathcal{M}}. \quad (42)$$

Then the second-order refocusing condition (18) implies

$$\mathcal{M}_{\alpha\beta} \Sigma_\alpha \Sigma_\beta = \mathcal{M}_{\alpha\beta} (B_{\alpha\beta}^\gamma + iC_{\alpha\beta}^\gamma) \Sigma_\gamma = 0, \quad (43)$$

while the first term in Eq. (40) was obtained from the double commutator,

$$[\Sigma_\alpha, [\Sigma_\beta, \Sigma_\delta]] = \Sigma_\alpha \Sigma_\beta \Sigma_\delta + \Sigma_\delta \Sigma_\beta \Sigma_\alpha - \Sigma_\alpha \Sigma_\delta \Sigma_\beta - \Sigma_\beta \Sigma_\delta \Sigma_\alpha.$$

Clearly, the first two terms in the corresponding product with $\mathcal{M}_{\alpha\beta}$ are zero due to the refocusing condition (43), while the remaining two terms cancel each other due to the antisymmetry of the matrix $\hat{\mathcal{M}}$.

The cancellation works essentially the same way for the terms involving symmetric matrices, even and odd derivatives of the real and imaginary parts of the correlator matrix $\hat{\mathcal{F}}(t)$, respectively, $\hat{\mathcal{F}}_1^{(2k)}(0)$ and $\hat{\mathcal{F}}_2^{(2k+1)}(0)$ (again, we use the assumption that ‘‘frozen’’ bath fluctuations are refocused). Thus, under most general conditions, the leading order term in the derivative expansion will be given by $\hat{\mathcal{F}}_2(0)$, which gives

$$\Gamma_2 \sim \Delta_2(0)\tau, \quad (44)$$

where $\Delta_2(t) \equiv \|\hat{\mathcal{F}}_2(t)\|$ is defined in analogy with $\Delta(t)$ but involves only the imaginary part of the correlator $\hat{\mathcal{F}}(t)$. Formally, this term is of the same order as that remaining after the first-order refocusing, Eq. (41). We note, however, that this contribution represents essentially quantum effects; for temperatures not small compared with the bath cutoff scale, $\beta\omega_c \lesssim 1$, it is expected to be small compared with $\Delta(t)$.

In practice, the leading-order contribution to the decoherence rate, Eq. (44), is often suppressed altogether. Indeed, the entire contribution of $\hat{\mathcal{F}}_2(t)$ to Eq. (40) is identically zero for the terms involving a single spin, as the nested commutator-anticommutator of Pauli matrices vanishes, $[\sigma_\alpha, \{\sigma_\beta, \sigma_\delta\}] = 0$ [the value $\beta=0$ is excluded from the implicit summation, cf. Eqs. (26) and (27)]. For more complicated systems (e.g., involving thermal bath correlated across several qubits), the matrix $\mathcal{F}(t)$ is expected to be symmetric as long as the bath is time-reversal invariant, that is, for real-valued spectral coupling function (24), $\hat{F}(\omega) = \hat{F}^*(\omega)$. In such cases all terms in the derivative expansion of the second-order contribution to the decoherence rate are sup-

pressed, which may result in an exponentially smaller value of Γ_2 for $\tau_0 \gg \tau$. Such a situation, where $\hat{\mathcal{F}}_2(t) \equiv 0$ and all orders in the derivative expansion with $\hat{\mathcal{F}}_1^{(k)}(0)$ are suppressed, are discussed in Sec. IV (see Figs. 6 and 7). Here the second-order contribution to the decoherence rate is seen to be small beyond the numerical precision already for $\tau_0/\tau \gtrsim 1$.

D. Initial decoherence

The spectrum of the decoherence rates associated with the modes around a frequency Ω_l , $l \neq 0$ is determined by the positions of the poles of the corresponding resolvent $(p - i\Omega_l - \hat{\Pi}_{l,l}^{[l]}(p))^{-1}$, in the vicinity of $p = i\Omega_l$. Because of the formal identity (37), $\hat{\Pi}_{l,l}^{[l]}(p) = \hat{\Pi}_{0,0}^{[0]}(p - i\Omega_l)$, the corresponding poles are distributed around $p = i\Omega_l$ in an identical fashion as those around $p = 0$. As a result, at time moments commensurate with the refocusing period, $t = \tau, 2\tau, 3\tau, \dots$, the contributions with all frequencies Ω_l add coherently, with the common set of decoherence rates $\{\gamma\}$ whose maximum is determined by Eqs. (41) and (44) depending on the order of the refocusing sequence.³⁶

The decoherence rates $\{\gamma\}$ determine the long-time exponential falloff of the refocusing accuracy. The corresponding prefactor determines the initial decoherence;²⁷ it can be found as the sum of the (nonsingular) matrix elements in Eqs. (38) and (39). For t sufficiently small, $\Gamma t \ll 1$, the correction due to the decoherence can be neglected, and the net contribution of a sector with given l can be found as the sum of the residues near $p = i\Omega_l$. For example, the total weight associated with the $l=0$ sector can be obtained from Eq. (39) as the coefficient in front of $p^{-1}R(0)$ at $\Gamma \ll p \ll \Omega$,

$$\hat{\kappa}_0 = (\hat{1} - \hat{\pi}'_0)^{-1} \left[\hat{1} + \sum_{m \neq 0} \frac{\hat{\Pi}_{0,m}^{[0]}(0)}{-i\Omega_m} \right], \quad \pi'_0 \equiv \left. \frac{d\hat{\Pi}_{0,0}^{[0]}(p)}{dp} \right|_{p=0}. \quad (45)$$

The weight of an $l \neq 0$ sector is obtained from Eq. (38),

$$\hat{\kappa}_l = \frac{\hat{\Pi}_{-l,0}^{[0]}(0)}{i\Omega_l} (\hat{1} - \hat{\pi}'_0)^{-1} \left[\hat{1} + \sum_{m \neq 0} \frac{\hat{\Pi}_{0,m}^{[0]}(0)}{-i\Omega_m} \right], \quad (46)$$

and the overall total, $\kappa = \sum_l \kappa_l$, is

$$\hat{\kappa} = \left[\hat{1} + \sum_{l \neq 0} \frac{\hat{\Pi}_{-l,0}^{[0]}(0)}{i\Omega_l} \right] (\hat{1} - \hat{\pi}'_0)^{-1} \left[\hat{1} + \sum_{m \neq 0} \frac{\hat{\Pi}_{0,m}^{[0]}(0)}{-i\Omega_m} \right]. \quad (47)$$

To quadratic order in powers of the perturbing Hamiltonian (the accuracy of the employed QKE), and to leading order in the derivative expansion [cf. Eq. (40)],

$$\begin{aligned} \hat{\Pi}_{0,m}^{[0]}(p) &= (A_m^{\text{tr}} J)_\alpha C_{\alpha\delta}^\gamma \\ &+ \sum_{m' \neq 0} \frac{[\hat{A}_{m'}^{\text{tr}} (J J^{\text{tr}} + \hat{\mathcal{F}}_1(0)) \hat{A}_{m-m'}]_{\alpha\beta}}{p - i\Omega_{m'}} C_{\alpha\alpha'}^\gamma C_{\beta\delta}^{\alpha'} \end{aligned} \quad (48)$$

$$\hat{\Pi}_{-m,0}^{[0]}(p) = (A_{m'}^{\text{tr}} J)_{\alpha} C_{\alpha\delta}^{\gamma} + \sum_{m' \neq 0} \frac{[\hat{A}_{m'}^{\text{tr}} (JJ^{\text{tr}} + \hat{\mathcal{F}}_1(0)) \hat{A}_{m-m'}]_{\alpha\beta}}{p + i\Omega_{m-m'}} C_{\alpha\alpha'}^{\gamma} C_{\beta\delta}^{\alpha'}. \quad (49)$$

Performing the expansion to quadratic order in J and linear order in \mathcal{F} and collecting various terms, we obtain for the overall coefficient (47), with the same accuracy,

$$(\hat{\kappa} - 1)_{\gamma\delta} = [\hat{q}^{\text{tr}} \hat{\mathcal{F}}_1(0) \hat{q}]_{\alpha\beta} C_{\alpha\alpha'}^{\gamma} C_{\beta\delta}^{\alpha'}, \quad (50)$$

where

$$\hat{q} \equiv \lim_{\epsilon \rightarrow +0} \int_0^{\infty} dt e^{-\epsilon t} \hat{Q}(t) = \sum_{m \neq 0} \frac{\hat{A}_m}{-i\Omega_m}. \quad (51)$$

Note that this expression was derived assuming solely order-one refocusing, yet the constant coefficients J^{α} give no contribution to quadratic order here. For a generic first- or second-order refocusing sequence $0 \neq \hat{q} \sim \tau$ and the initial decoherence can be estimated as

$$\|\hat{\kappa} - 1\| \sim \Delta(0) \tau^2. \quad (52)$$

For sequences which produce time-reversal symmetric evolutions, $\hat{Q}(t) = \hat{Q}(-t)$, the Fourier components are real-valued, $\hat{A}_m = \hat{A}_{-m}$, and the sum (51) vanishes identically. In such cases the initial decoherence is smaller, and it is determined by higher derivatives of the bath correlation function, e.g.,

$$\|\hat{\kappa} - 1\|_{\text{symm}} \sim |\Delta''(0)| \tau^4 \quad (53)$$

for the symmetric sequence in Fig. 7.

So far we only considered the terms $\sim R(0)$ which depend on the initial conditions for the density matrix. The remaining terms in the right-hand side of Eqs. (39) and (38) provide an additional source of errors, as these terms are responsible for establishing the correlations characteristic for the stationary state at large t ; they are required to vanish at $t \rightarrow 0$. In real time the corresponding contributions come with the prefactors $1 - e^{(i\Omega_l - \gamma)t}$, small at commensurate time moments $t = \tau, 2\tau, \dots$, because the decoherence rates γ are small. Additional smallness arises because the refocusing tends to average out the correlations which would normally appear as the equilibrium is reached. Therefore, we expect these contributions to be quartic, beyond the accuracy of the present calculation.

IV. EXAMPLE: SINGLE-SPIN KINETICS

In this section we illustrate the derived general expressions on an example of a single qubit (spin) driven by classical fluctuating fields. Specifically, we use Gaussian random fields $b_{\alpha}(t)$ along one (x) or all three directions, with the correlators

$$\langle b_{\alpha}(t) \rangle = 0, \quad \langle b_{\alpha}(t) b_{\beta}(t') \rangle = \delta_{\alpha\beta} b_0^2 e^{-t^2/(2\tau_0^2)}, \quad (54)$$

where b_0 is the rms amplitude of the random field and τ_0 is the correlation time. The correlated field is generated using

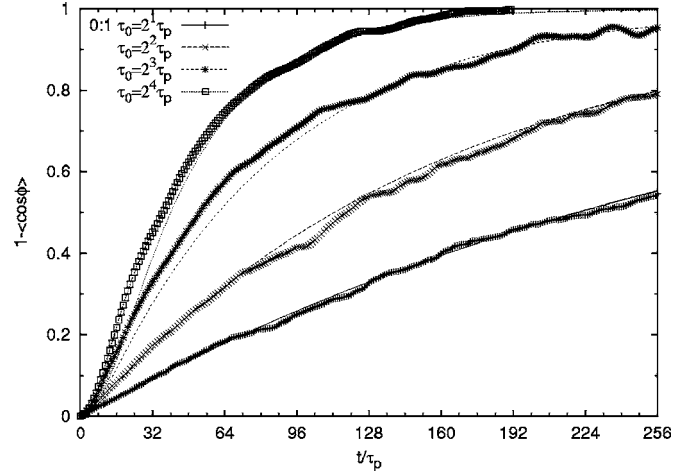


FIG. 1. “Refocusing error” (specifically, three times the deviation of the average fidelity for the spin to remain in the initial state from one), in the absence of refocusing. The Gaussian random field is applied along the x axis only. For different curves, it has the same rms amplitude b_0 but different values of the correlation time τ_0 [see Eq. (54)]. Symbols show the results of simulation averaged over 900 samples of the random field; lines show the corresponding exact results (55) and (56) which for $t \gg \tau_0$ are also very close to the QKE result (not shown). See text for other notations.

the spectral filter based on the fast Fourier transformation of a sequence of originally uncorrelated Gaussian random numbers. As a result, $b_{\alpha}(t)$ are actually periodic over the simulation interval (which is always long compared to τ_0).

The density matrix (6) is described by the three-component vector \mathbf{R} , $R^2 = 1$, whose quantum dynamics is described by the Bloch equation,

$$\dot{\mathbf{R}} = [\mathbf{B}(t) \times \mathbf{R}],$$

where $B_{\alpha}(t) = V_{\alpha}(t) + b_{\alpha}(t)$ is the net magnetic field [see Eqs. (2) and (4)]. In terms of the vector \mathbf{R} , the spin evolution in a given classical field is a rotation; the goal of refocusing is to reduce the total rotation angle ϕ . The average fidelity of the refocusing, the probability for the qubit to remain in the original state, averaged over initial conditions, is equal to $1 - (1 - \langle \cos \phi \rangle)/3$.

In Fig. 1 we show the results of time-dependent simulations for a single spin driven by a one-component random field with four different values of the correlation time τ_0 . We plot the quantity $1 - \langle \cos \phi \rangle$, proportional to the deviation of the average fidelity for the spin to remain in the same state from one, as a function of time t in units of τ_p , a time scale equal to the interval between consecutive refocusing pulses. The rms amplitude of the random field is the same for all curves (in fact, everywhere throughout this work), $b_0 = 0.0355/\tau_p$. The numerical data are compared with the exact analytical solution,

$$1 - \langle \cos \phi(t) \rangle = 1 - e^{-\langle \phi^2(t) \rangle / 2}, \quad \phi(t) = \int_0^t b_x(t') dt', \quad (55)$$

$$\frac{\langle \phi^2 \rangle}{2} = b_0^2 \tau_0^2 (\pi^{1/2} x \operatorname{erf} x + e^{-x} - 1), \quad x = \frac{t}{\sqrt{2} \tau_0}. \quad (56)$$

For long-time asymptotics we obtain

$$\langle \cos \phi(t) \rangle \rightarrow e^{b_0^2 \tau_0^2 e^{-\gamma_{\text{exact}} t}}, \quad \gamma_{\text{exact}} = b_0^2 \tau_0 (\pi/2)^{1/2}. \quad (57)$$

To make a connection to the quantum kinetic equation, we notice that in the simulations we perform the averaging over the classical random fields, instead of that over the quantum dynamics of the thermal bath. As a result, the correlation matrix $\mathcal{F}_{\alpha\beta}(t-t') = \langle b_\alpha(t) b_\beta(t') \rangle$ is explicitly real-valued, $\hat{\mathcal{F}}_2(t) = 0$. In the absence of the control fields, the Laplace-transformed QKE (28) is

$$\tilde{\mathbf{R}}(p) = [p - \hat{\Pi}(p)]^{-1} \mathbf{R}(0), \quad (58)$$

$$\Pi_{\gamma\delta}(p) = J_\alpha e^{\alpha\delta\gamma} + \tilde{\mathcal{F}}_{\gamma\delta}(p) - \delta_{\gamma\delta} \tilde{\mathcal{F}}_{\alpha\alpha}(p). \quad (59)$$

With $J_\alpha = 0$, and for the random field along the x axis only, the exponent and the prefactor of the exact long-time asymptotics can be calculated to quadratic order in the noise amplitude by expanding the resolvent of Eq. (58) around the point $p=0$,

$$\tilde{\mathbf{R}}(p) \approx [p - p\hat{\Pi}'(0) - \hat{\Pi}(0)]^{-1} \mathbf{R}(0).$$

This gives in real time [cf. Eq. (57)]

$$\langle \cos \phi \rangle \rightarrow (1 - b_0^2 \tau_0^2)^{-1} e^{-\gamma t}, \quad \gamma = \frac{\gamma_{\text{exact}}}{1 - b_0^2 \tau_0^2}.$$

The simulations with refocusing were performed using a symmetric length-8 pulse sequence “8p” (XYXYXYXY), as well as a set of “concatenated” pulse sequences, “4c” (XYXY), “8c” (XYXYXYXY), “16c” (XYXYXYXYXYXYXYXY), etc., where X is a π -pulse along the x direction, \bar{X} is a negative- π pulse, and the longer sequences are obtained recursively by ramping the signs of the pulses. This concatenation procedure is somewhat similar but differs from that used in Ref. 37.

We used the Gaussian pulses,³⁸ as well as the first- and second-order self-refocusing π -pulses, S_L and Q_L , respectively, designed by the authors previously.²⁰ Pulses S_L , $L=1,2$ are analogous to the first-order Hermitian pulses³⁹ but they were constructed so that the amplitude of the signal (along with the derivatives up to $2L$ th) turn to zero at the ends of the interval of the duration τ_p . Pulses Q_L , $L=1,2$ are similarly designed one-dimensional second-order self-refocusing pulses.

The order of the sequences with the particular pulses and for different directions of the applied constant field are listed in Table I. The sequence 8p has the duration $\tau = 8\tau_p$, and so the Fourier expansion of the corresponding evolution operator $Q(t)$ starts with the frequency $\Omega = 2\pi/(8\tau_p)$. Similarly, for sequences 4c, 8c, ..., the Fourier expansion starts with $2\pi/(4\tau_p)$, $2\pi/(8\tau_p)$, etc. However, due to the structure of these sequences, the low-frequency Fourier coefficients for sequences in the nc series with larger n turn out to be very small numerically, and scaling as $\sim \Omega^2$, as illustrated in Figs.

TABLE I. Order of the refocusing sequences (rows) with different pulse shapes (columns), depending on the direction of the applied constant field. The order values listed represent the number of canceled terms in the cumulant expansion (11) of the evolution operator with the bath variables replaced by c numbers. “G” stands for Gaussian pulses (Refs. 38 and 39), S_L and Q_L , $L=1,2$ are first- and second-order one-dimensional self-refocusing pulses, respectively, with up to $2L-1$ derivatives vanishing at the ends of the interval (Ref. 20). The superscripts * or ** denote that the first nonvanishing cumulant is “small” or “very small” numerically (smaller by some two and four orders of magnitude, respectively, compared to what is expected from naive scaling). The expansion was done numerically keeping ten orders in the time-dependent perturbation theory as explained in Ref. 20. See text for definitions of the sequences.

Seq/pulse	1: $B_x \neq 0$			2: $B_z \neq 0$			3: $B_x, B_y, B_z \neq 0$		
	G	S_L	Q_L	G	S_L	Q_L	G	S_L	Q_L
4c	0	2	2	0	1	2	0	1	1
8c	2	4	6	1	3	5*	1	1	1
16c	2	4	6*	2	6*	8*	1	1	1
32c	2	4*	6**	4*	8**	≥ 10	1	1	1
64c	2	4**	6**	4**	≥ 10	≥ 10	1	1	1
8p	1	1	3	1	1	3	1	1	2

2–5. As a result, for relatively fast fluctuations (small τ_0) the long-time refocusing accuracy for these sequences can be substantially better than that of equal or shorter ordinary sequences (compare the slopes with $\tau_0 = 2^2 \tau_p$ in Figs. 6 and 7). We also note the suppressed high-frequency tail of the spec-

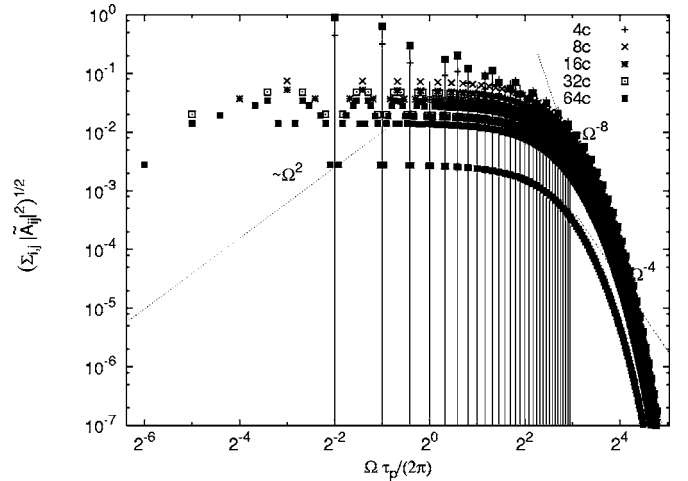


FIG. 2. The Frobenius norm of the matrices \hat{A}_m [Fourier transform of the evolution matrices $\hat{Q}(t)$, see Eq. (15)] with frequencies $\Omega_m = 2\pi m/\tau_p$ for sequences nc , $n=4,8,\dots,64$ with Gaussian π -pulses. The width of a pulse is chosen to be $0.05\tau_p$ so that the discontinuity at the ends of the interval is numerically negligible, which results in a steep cutoff at high frequencies. Vertical lines mark the spectral features of the parent sequence 4c, which dominate the spectrum of all higher-order sequences. Thin dotted lines guide the eye with the slope corresponding to power laws as indicated.

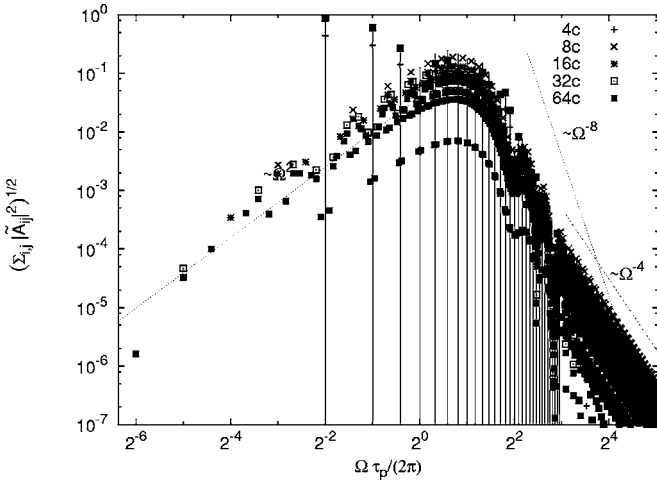


FIG. 3. As in Fig. 2 for first-order self-refocusing pulses S_1 .

tra in Fig. 5 which illustrates the advantage of the pulses Q_2 designed²⁰ specifically for reduced spectral width.⁴⁰

Figures 6 and 7 show the refocusing error, $1 - \langle \cos \phi \rangle$, with the refocusing pulses present as described in the captions. The amplitudes of the fluctuating field $b_\mu(t)$ (along one or three directions) are the same as for the data in Fig. 1, but the vertical scale here is reduced by some two orders of magnitude. This totally hides the curvature of the plots a few correlation times away from the origin, which allows a linear fit,

$$1 - \langle \cos \phi \rangle = A + Bt/\tau_p. \quad (60)$$

The coefficients represent the initial decoherence proportional to the intercepts A with the vertical axis, and the decoherence rate proportional to the slopes B . We note that the random field used in the simulations is periodic with the period $T=256\tau_p$; as a result the overall error is almost entirely compensated towards the end of the simulation inter-

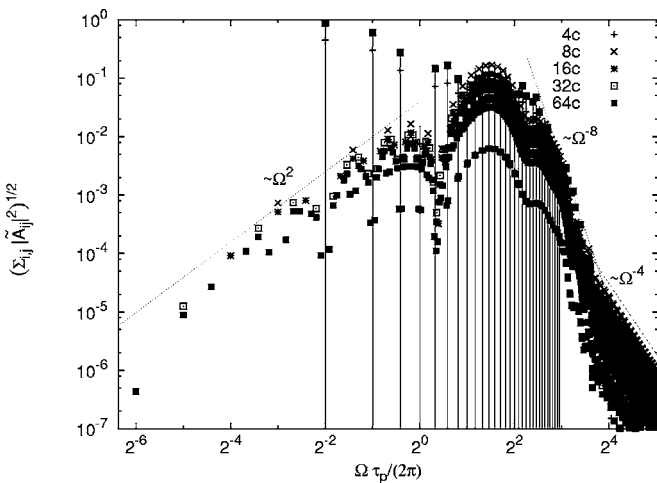


FIG. 4. As in Figs. 2 and 3 with second-order pulses Q_1 . Note a suppression of the low-frequency part of the spectrum compared with lower-order pulses.

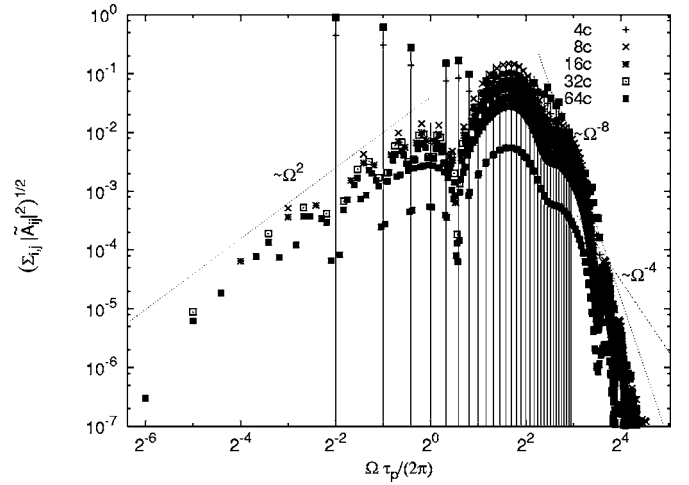


FIG. 5. As in Figs. 2–4 for second-order pulses Q_2 . These shapes vanish at the ends of the interval along with the first three derivatives, which suppresses the high-frequency part of the spectrum.

val. Respectively, only the data further than $\Delta t = 3\tau_0$ from the ends of the interval were used in the fits.

The pulse shapes and the fluctuating fields chosen for simulations in Figs. 6 and 7 are such that the pulse sequences provide at least second-order refocusing. With solely classical correlations, $\hat{\mathcal{F}}_2(t)=0$ and $\hat{\mathcal{F}}_1(t)$ symmetric, the decoherence rate is expected to go down dramatically with increasing τ_0 . This is exactly what is seen in Figs. 6 and 7: already at $\tau_0 \geq \tau$ the real-time graphs look almost horizontal and the corresponding slopes B scale down rapidly with increasing τ_0 , so that they become too small for the numerical precision of the calculation.

While the sequence 8p is explicitly symmetric with respect to the origin, the sequences nc are not. As a result, with slow fluctuations $\tau_0/\tau \geq 1$, the initial decoherence for the latter sequence tends to a constant value, as can be seen from the intercepts A in Fig. 6. On the other hand, the intercepts tend to be much smaller in Fig. 7, where the symmetric sequence 8p was used. This results in an excellent overall refocusing accuracy.

We have also simulated the spin dynamics under the 4c sequence in the presence of the fluctuating magnetic field along the z direction, using Gaussian, S_1 , and Q_1 pulses which provide zeroth-, first-, and second-order refocusing, respectively (not shown). The decoherence rates in the three cases are seen as proportional to τ_0 , independent of τ_0 , and vanishing rapidly with $\tau_0 \geq \tau$, as expected from the analytic calculations.

V. CONCLUSIONS

In this work we discussed the kinetics of a quantum system subject to a pulse-based control field of arbitrary shape. We concentrated on the simplest case of dynamical decoupling, or refocusing, where the only goal is to cancel any evolution due to intrinsic or extrinsic couplings. We solved the problem in the approximation of a non-Markovian quan-

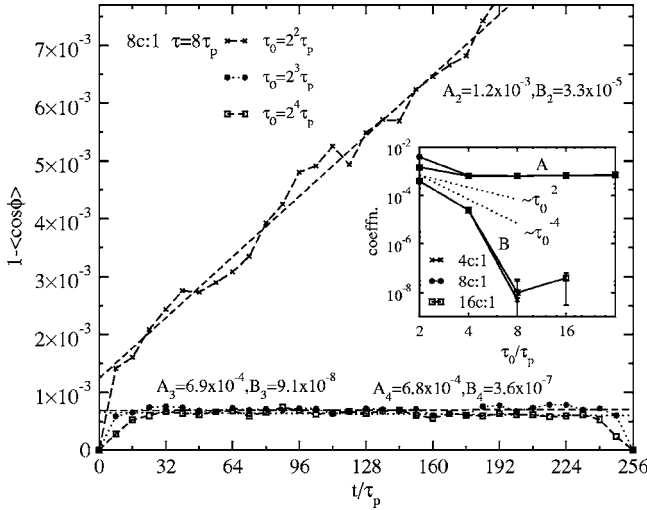


FIG. 6. Refocusing error with the fluctuating magnetic field along the x axis as in Fig. 1, but now in the presence of refocusing sequence 8c with pulses Q_1 (order 2, see Table I). Symbols represent the data averaged over 900 realizations of noise and dashes are the linear fits [Eq. (60)] for data further than $\Delta t = 3\tau_0$ from the ends of the interval. The inset shows the fit coefficients for sequences 4c, 8c, and 16c as a function of the correlation time τ_0 . Dotted lines on the inset indicate the slope corresponding to the power laws as indicated. The decoherence rate (proportional to the slopes B) is reduced dramatically for the correlation time τ_0 exceeding the duration of the sequence, $\tau = n\tau_p$ for sequence nc . Yet the refocusing error does not disappear altogether because of the initial decoherence (proportional to the intercept A) which does not vanish with increased noise correlation time τ_0 for these nonsymmetric sequences [see Eq. (52)]. The data on the inset also show that the refocusing accuracy is not improved with the longer sequences of order above second, but it also does not worsen even for small τ_0/τ (the low-frequency harmonics \hat{A}_m are suppressed, see Fig. 4). The refocusing errors are strongly suppressed near the end of the interval because the fluctuating field used in the calculation is periodic with the period $T = 256\tau_p$.

tum kinetic equation, which limits the accuracy to quadratic order in powers of the perturbations, but considered the evolution due to the control fields exactly. The equations correctly represent long-time dissipative dynamics. The corresponding decoherence rates and the prefactor are evaluated to second order in powers of the small parameter, the evolution amplitude due to the perturbation over the period of the refocusing sequence.

We demonstrated that higher-order refocusing sequences can be very effective in canceling the decoherence effects of the couplings to slow external degrees of freedom. If in the absence of control the decoherence rate due to the bath with the characteristic correlation time τ_0 is Γ_0 [Eq. (30)], with sufficiently fast order-one period- τ refocusing ($\tau \lesssim \tau_0$), the decoherence rate can be reduced by a factor of $\sim (\tau/\tau_0)$ [Eq. (41)]. This reduced value accounts for both dissipative and reactive terms and is dominated by the latter, as long as the driven dynamics is in the spectral gap of the thermal bath. With second-order refocusing, the decoherence rate is further reduced, as it is now determined only by the quantum part of the bath correlator [Eq. (44)]. With the bath coupling time-

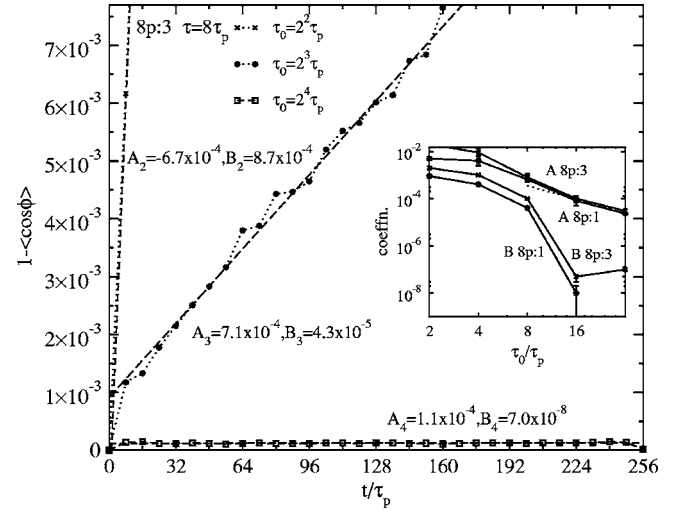


FIG. 7. As in Fig. 6 but for the sequence 8p (pulses Q_1) and for the magnetic field fluctuating in all three directions, Eq. (22). Amplitude b_0 along each direction and other simulation parameters are as in Fig. 6. Inset shows the linear fit coefficients for this sequence with the magnetic field fluctuating in one (8p:1) and all three (8p:3) directions. The effective decoherence rate for the fastest fluctuations, $\tau_0 = 4\tau_p$, is bigger than those in the simulations with nc sequences. However, with $\tau_0 > \tau = 8\tau_p$, the decoherence rate (slope B) again goes down dramatically, while the initial decoherence also scales down *quadratically* with increasing τ_0 , resulting in a superior refocusing accuracy.

reversal invariant, additional cancellations are possible, which may ultimately lead to the decoherence rate (in the QKE order) smaller than any power of the adiabaticity parameter τ/τ_0 .

As noted on many occasions in NMR literature, symmetric refocusing sequences provide for additional cancellations in the evolution operator and often provide superior refocusing accuracy.⁴¹ Here we show that the symmetry is also crucial for reducing the initial decoherence, an effective dephasing which occurs at the beginning of the refocusing sequence. While generic first- or higher-order control sequences result in an initial decoherence proportional to the square of the amplitude of the fluctuating fields, $\sim \Gamma_0^2/\tau_0$ [Eq. (52)], with symmetric sequences this leading-order contribution is canceled, which produces an additional reduction by a power of the adiabaticity parameter τ/τ_0 .

We illustrated these cancellations by simulations of a single qubit in the presence of a classical fluctuating magnetic field. Our simulations suggest that using nonsymmetric refocusing sequences of an order higher than 2 does little to improve the decoherence rate of the controlled system. Unlike the formulas that target the scaling, the simulations also illustrate the actual magnitude of the achieved reduction in decoherence.

In this work we concentrated on the dynamics of a relatively small quantum system and ignored the scaling of the decoherence rates with the size of the system. For example, the estimate Eq. (44) can be rewritten as an upper bound on the decoherence rate, in which case it contains an additional factor of N , the number of levels in the controlled system. Further studies with specific models of bath coupling are

needed to understand in what cases this scaling with N can be suppressed. Present estimates are useful for small, few-qubit systems, or for situations where the thermal bath does not induce long-range correlations between distant qubits. We plan to analyze the scaling with the system size and the range of correlations in the thermal bath in a future publication. Another planned extension of this work is to analyze the quantum kinetics of a system and ways to reduce deco-

herence during the operation of a quantum algorithm, without the assumptions that the control fields are periodic.

ACKNOWLEDGMENTS

We would like to thank Mark Dykman and Daniel Lidar for numerous illuminating discussions, and Kaveh Khodjasteh for insightful comments on the manuscript.

*Present address: Department of Physics & Astronomy, University of Southern California, Los Angeles, California 90089, USA.

¹C. P. Slichter, *Principles of Magnetic Resonance*, 3rd ed. (Springer-Verlag, New York, 1992).

²P. Hodgkinson and L. Emsley, *Prog. Nucl. Magn. Reson. Spectrosc.* **36**, 201 (2000).

³L. M. K. Vandersypen and I. L. Chuang, *Rev. Mod. Phys.* **76**, 1037 (2004).

⁴E. L. Hahn, *Phys. Rev.* **80**, 580 (1950).

⁵U. Haeberlen and J. S. Waugh, *Phys. Rev.* **175**, 453 (1968).

⁶U. Haeberlen and J. S. Waugh, *Phys. Rev.* **185**, 420 (1969).

⁷A. Pines and J. S. Waugh, *J. Magn. Reson.* (1969-1992) **8**, 354 (1972).

⁸A. Pines and J. S. Waugh, *Phys. Lett.* **47A**, 337 (1974).

⁹L. Viola and S. Lloyd, *Phys. Rev. A* **58**, 2733 (1998).

¹⁰D. Vitali and P. Tombesi, *Phys. Rev. A* **59**, 4178 (1999).

¹¹L. Viola, E. Knill, and S. Lloyd, *Phys. Rev. Lett.* **82**, 2417 (1999).

¹²L. Viola, S. Lloyd, and E. Knill, *Phys. Rev. Lett.* **83**, 4888 (1999).

¹³L. Viola, E. Knill, and S. Lloyd, *Phys. Rev. Lett.* **85**, 3520 (2000).

¹⁴D. Vitali and P. Tombesi, *Phys. Rev. A* **65**, 012305 (2002).

¹⁵C. Uchiyama and M. Aihara, *Phys. Rev. A* **66**, 032313 (2002).

¹⁶M. S. Byrd and D. A. Lidar, *Phys. Rev. A* **67**, 012324 (2003).

¹⁷K. Shiokawa and D. A. Lidar, *Phys. Rev. A* **69**, 030302(R) (2004).

¹⁸L. Faoro and L. Viola, *Phys. Rev. Lett.* **92**, 117905 (2004).

¹⁹P. Facchi, S. Tasaki, S. Pascazio, H. Nakazato, A. Tokuse, and D. A. Lidar, *Phys. Rev. A* **71**, 022302 (2005).

²⁰P. Sengupta and L. P. Pryadko, *Phys. Rev. Lett.* **95**, 037202 (2005).

²¹O. V. Konstantinov and V. I. Perel, *Zh. Eksp. Teor. Fiz.* **39**, 197 (1960).

²²E. B. Davies, *Commun. Math. Phys.* **39**, 91 (1974).

²³M. I. Dykman, *Phys. Status Solidi B* **88**, 463 (1978).

²⁴R. Alicki, *Phys. Rev. A* **40**, 4077 (1989).

²⁵A. G. Kofman and G. Kurizki, *Phys. Rev. Lett.* **87**, 270405 (2001).

²⁶A. G. Kofman and G. Kurizki, *Phys. Rev. Lett.* **93**, 130406 (2004).

²⁷G. Falci, A. D'Arrigo, A. Mastellone, and E. Paladino, *Phys. Rev. Lett.* **94**, 167002 (2005).

²⁸M. I. Dykman, *Fiz. Nizk. Temp.* **5**, 186 (1979) [*Sov. J. Low Temp. Phys.* **5**, 89 (1979)].

²⁹B. Ischi, M. Hilke, and M. Dubé, *Phys. Rev. B* **71**, 195325 (2005).

³⁰P. W. Shor, *Phys. Rev. A* **52**, R2493 (1995).

³¹H. Rabitz, D. Regina Vivie-Riedle, M. Motzkus, and K. Kompa, *Science* **288**, 824 (2000).

³²R. J. Levis, G. M. Menkir, and H. Rabitz, *Science* **292**, 709 (2001).

³³Y. Ohtsuki, *J. Chem. Phys.* **119**, 661 (2003).

³⁴J. S. Waugh, L. M. Huber, and U. Haeberlen, *Phys. Rev. Lett.* **20**, 180 (1968).

³⁵J. S. Waugh, C. H. Wang, L. M. Huber, and R. L. Vold, *J. Chem. Phys.* **48**, 652 (1968).

³⁶When reporting preliminary results of this work in the conclusion of Ref. 20, we erroneously stated that “only the dynamics in the slow sector is protected by the refocusing.” While the latter statement should be disregarded, it does not reduce the validity of other results of Ref. 20.

³⁷K. Khodjasteh and D. A. Lidar, *Phys. Rev. Lett.* **95**, 180501 (2005).

³⁸C. Bauer, R. Freeman, T. Frenkiel, J. Keeler, and A. J. Shaka, *J. Magn. Reson.* (1969-1992) **58**, 442 (1984).

³⁹W. S. Warren, *J. Chem. Phys.* **81**, 5437 (1984).

⁴⁰P. Borgnat, A. Lesage, S. Caldarelli, and L. Emsley, *J. Magn. Reson., Ser. A* **119**, 289 (1996).

⁴¹M. Mehring, *Principles of High-resolution NMR in Solids* (Springer-Verlag, New York, 1983).